Vacuum-UV fluorescence spectroscopy of SiF4SiF4 in the range 10–30 eV

Biehl, H.; Boyle, Kenneth; Seccombe, D. P.; Smith, D. M.; Tuckett, R. P.; Yoxall, K. R.; Baumgärtel, H.; Jochims, H. W.

DOI:
10.1063/1.474437

Vacuum-UV fluorescence spectroscopy of SiF_4 in the range 10–30 eV

H. Biehl, K. J. Boyle, D. P. Seccombe, D. M. Smith,[a] R. P. Tuckett,[b] and K. R. Yoxall
School of Chemistry, University of Birmingham, Edgbaston, Birmingham B15 2TT, United Kingdom

H. Baumgärtel and H. W. Jochims
Institut fur Physikalische und Theoretische Chemie, Freie Universitat Berlin, Takustrasse 3, 14195 Berlin, Germany

(Received 14 March 1997; accepted 10 April 1997)

The vacuum-UV and visible spectroscopy of SiF_4 using fluorescence excitation and dispersed emission techniques is reported. The fluorescence excitation spectrum has been recorded following excitation with synchrotron radiation from the BESSY 1, Berlin source in the energy range 10–30 eV with an average resolution of $\sim$ 0.05 eV. By comparison with vacuum-UV absorption and electron energy loss spectra, all the peaks in the Rydberg spectra that photodissociate to a fluorescing state of a fragment have been assigned. Dispersed emission spectra have been recorded at the energies of all the peaks in the excitation spectra. Four different decay channels are observed: (a) SiF_3 fluorescence in the range 380–650 nm for photon energies around 13.0 eV, (b) SiF_2 $\tilde{a}\,^3B_1$–$\tilde{X}\,^1A_1$ phosphorescence in the range 360–440 nm for photon energies in the range 15.2–18.0 eV, (c) SiF_2 $\tilde{A}\,^1B_1$–$\tilde{X}\,^1A_1$ fluorescence in the range 210–270 nm for photon energies in the range 17.0–20.0 eV, and (d) emission from the $\tilde{D}\,^2A_1$ state of SiF_4^+ predominantly in the range 280–350 nm for photon energies greater than 21.5 eV. These assignments are confirmed by action spectra in which the excitation energy of the vacuum-UV radiation is scanned with detection at a specific (dispersed) wavelength. Using the single-bunch mode of the synchrotron, lifetimes of all the emitting states have been measured. The lifetimes of the unassigned emitting state in SiF_3, the $\tilde{A}\,^1B_1$ state of SiF_2, and the $\tilde{D}\,^2A_1$ state of SiF_4^+ are 3.9 $\pm$ 0.7, 11.2 $\pm$ 1.5, and 9.16 $\pm$ 0.02 ns, respectively. This is the first measurement of the lifetimes of these excited states in SiF_3 and SiF_2. The decay from the $\tilde{a}\,^3B_1$ state of SiF_2 has a fast component of 2.6 $\pm$ 0.4 ns. We conclude that the lifetime of the $\tilde{a}\,^3B_1$ state of SiF_2 is either as low as 2.6 ns or too high ($\tau > \sim$200 ns) to measure with the timing profile of the single-bunch mode of BESSY 1. If the latter interpretation is correct, as seems likely for a spin-forbidden phosphorescence to the $^1A_1$ ground state, the 2.6 ns component could be the lifetime of intersystem crossing from higher vibrational levels of the $\tilde{a}\,^3B_1$ state of SiF_2 into its ground state. © *1997 American Institute of Physics.* [S0021-9606(97)02727-X]

I. INTRODUCTION

There is considerable interest in the plasma dry etching of silicon wafers for the fabrication of microelectronic devices. Although fluorine-containing gases (e.g., CF_4, C_2F_6) have been used for many years to etch silicon, there is still uncertainty as to which volatile products desorb from the silicon surface and hence play a role in the etching process. Etching proceeds by the formation of volatile products through ion-stimulated reaction between the wafer surface and reactive neutral species generated by a radio-frequency glow discharge. The characteristic glow from these plasmas is due to emission from electronically excited species (e.g., free radicals and molecular ions). Optical emission spectroscopy has proved to be a powerful analytical tool to identify such species present in the plasma, and it is now well established that the SiF_2 molecule plays an important part in the etching process.[1–3] The electronic spectroscopy of SiF_2 is now well understood by a variety of techniques, including absorption,[4] emission,[5] laser-induced fluorescence, and phosphorescence,[2,6] and multiphoton ionization.[7] There have also been a number of high-quality *ab initio* calculations performed on this molecule,[8] however there is limited information on the lifetimes of the excited states of SiF_2. By contrast, the spectroscopy of the SiF_3 radical in the gas phase is very poorly understood, and there has only been one report of a dispersed emission spectrum.[9] Mainly because an unambiguous analytical sensor for the SiF_3 radical has not been established, it is still unknown whether this radical plays an important role in the fluorine etching of silicon.

In radio-frequency discharges of the kind used in plasma etching, fragment radicals and ions are created in an ill-defined manner by electrons whose energies include the wide range 5–30 eV. In order to understand the spectroscopy of these species in more detail, we have used the more controllable method of photon excitation of SiF_4. Tunable vacuum-UV radiation from a synchrotron source is used to cover the same energy range as the plasma electrons. In the experiments reported here, we disperse the fluorescence induced by tunable vacuum-UV radiation from the BESSY 1 synchrotron source through a (secondary) monochromator. Such experiments are commonly performed using fixed-energy metastable atom and discharge lamp sources, but are

[a]Present address: Department of Chemistry, University of Southampton, Highfield, Southampton SO17 1BJ, UK.
[b]Author to whom correspondence should be addressed.

 0021-9606/97/107(3)/720/10/$10.00

rare using the lower intensity tunable dispersed radiation from a second-generation synchrotron source. Our results complement our earlier study on SiF_4[10] performed at the Daresbury Laboratory synchrotron source (SRS) in the United Kingdom, where we only used photon energies greater than 20 eV giving rise to emission in the parent ion SiF_4^+ and detected undispersed fluorescence. Our present work also substantially extends that of Suto *et al*. who measured absolute photoabsorption and fluorescence cross sections for SiF_4 over the range 10–25 eV.[11] They also observed dispersed emission spectra but only at a few defined energies using a capillary discharge lamp source.[9,11] Using the single-bunch mode of the synchrotron source, we also measure the lifetimes of all the species produced in excited, fluorescing states from SiF_4 photoexcited in the vacuum-UV in the range 10–30 eV.

II. EXPERIMENT

Experiments were performed at the BESSY 1 synchrotron storage ring in Berlin using an apparatus described elsewhere.[12] A 1.5 m normal-incidence monochromator (range 7–25 eV, best resolution 0.03 nm) attached to the 800 MeV electron storage ring provided a source of tunable vacuum-UV radiation. A removable LiF window mounted close to the exit slit of the monochromator could be used to eliminate second-order radiation for spectra recorded at excitation wavelengths longer than ~110 nm. Radiation from the exit slit of this primary monochromator passed through a small chamber (pumped by a Balzers TPU 180 magnetically-balanced turbo pump to provide differential pumping between this monochromator and the interaction region), and via a 1 mm slit into a small brass cube of side 20 mm which was cryogenically pumped by a large liquid-nitrogen trap. The sample vapor effused into this interaction region giving a typical pressure within the first chamber of $\sim 2\times10^{-5}$ Torr; the pressure within the brass cube was higher although it was not possible to measure it directly. The induced fluorescence passed through a quartz window and was dispersed by a small 20 cm focal length monochromator (Jobin Yvon H20UV). This secondary monochromator had no entrance slit and a fixed exit slit. In the spectroscopic experiments using the multibunch, quasi-continuous mode of the synchrotron, fluorescence was detected by a photon-counting EMI 9789 QB photomultiplier tube cooled to 248 K. The effective range of this secondary monochromator was then 190–450 nm, the low wavelength being limited by the quartz optics, the high wavelength by the blaze of the grating (~300 nm) and the quantum efficiency range of the bi-alkali photomultiplier tube. The lifetime experiments using the single-bunch mode of the synchrotron utilised a red-enhanced Hamamatsu R6060 photomultiplier tube cooled to ~280 K and a Jobin Yvon H20VIS secondary monochromator (grating blaze ~450 nm), both of which improved the sensitivity of this apparatus for wavelengths greater than 400 nm. The multibunch experiments were performed with a 1.0 mm exit slit on the secondary monochromator, corresponding to an optical resolution of ~4 nm. In order to maximize signal, the lifetime experiments used no exit slit at all, giving a resolution of ~50 nm.

In the multibunch mode, the following three experiments were possible. First, fluorescence excitation spectroscopy, in which the secondary monochromator was set to zero order and the primary monochromator was scanned. Second, action spectroscopy, in which the secondary monochromator was set to a specific fluorescence wavelength (± 4 nm) and the primary monochromator was scanned. Third, dispersed fluorescence spectroscopy, in which the induced fluorescence was dispersed for a fixed photoexcitation energy between 7 and 25 eV. None of the spectra have been corrected for the variation in sensitivity of the primary and secondary monochromators with wavelength. The scanning of both monochromators and the data collection were controlled using a personal computer. Both primary and secondary monochromators were calibrated using the $N_2^+ B\ ^2\Sigma_u^+ - X\ ^2\Sigma_g^+(0,0)$ emission band at 391 nm whose threshold for production is 18.76 eV.[13] In the single-bunch mode, lifetimes of the emitting states were measured in the following manner. The VUV excitation wavelength (λ_1) and the emission wavelength (λ_2) were defined, with wide slits used in both primary and secondary monochromators in order to maximize the signal intensity. After shaping and discrimination, fluorescence pulses from the Hamamatsu photomultiplier tube (rise time ~1.5 ns) were used as the start signal for an Ortec 567 time-to-amplitude converter. The synchrotron bunch marker (20 ps pulses every 208 ns, the transit time of electrons around the storage ring) were also shaped and discriminated, and used as the stop signal. The resulting decay data were collected in real time using a multichannel analyser card mounted in a 386 personal computer. An absolute time calibration was provided by an Ortec 462 time calibrator. The lifetime of the $B\ ^2\Sigma_u^+$ state of N_2^+ was measured to be 60 ± 1 ns. This value is in agreement with that given in the literature,[13] confirming that collisional quenching makes no contribution to the rate of decay of the fluorescence signal for shorter lifetimes at the pressures used in these experiments. The SiF_4 sample (Alpha, 99.99%) was taken direct from a gas bottle without purification.

Preliminary experiments were performed at the U.K. synchrotron source at Daresbury with *undispersed* detection of the fluorescence.[12] Dispersed vacuum-UV radiation from a 5 m McPherson normal-incidence monochromator (range 8–30 eV, optimum resolution 0.01 nm) crossed an effusive flow of SiF_4 vapor at a pressure of $\sim 1\times10^{-4}$ Torr. Fluorescence induced at the interaction region was focussed through a Spectrocil B quartz window using an aluminium coated $f=75$ mm spherical concave mirror onto an EMI 9883 QB photomultiplier tube (range 190–650 nm) maintained at 298 K and used in the photon-counting mode. Optical filters could be inserted in front of the photomultiplier tube to isolate different emission bands. Fluorescence excitation spectra were recorded at a resolution of 0.1 nm (~0.02 eV at 15 eV) using the quasi-continuous multibunch mode of the synchrotron, and lifetimes were recorded using the single-bunch mode (200 ps pulses every 320 ns) with similar

electronics to the BESSY 1 experiments. The main advantage of this apparatus compared to that used in Berlin is that it is sensitive to visible radiation with $\lambda > \sim 450$ nm, whereas the Berlin apparatus used for the multibunch experiments has very limited sensitivity in this region of the visible spectrum. The Daresbury apparatus does, however, have two principal disadvantages. The region of the UV/visible spectrum where fluorescence is observed can only be determined very approximately by the use of broad band or cut-on filters, because the fluorescence is not dispersed through a secondary monochromator. In addition, second-order radiation in the range 11–18 eV from the grating of the McPherson primary monochromator was significant at the time our experiments were made. Very strong, nonresonant emission from the $\tilde{D}\ ^2A_1$ state of SiF_4^+ (threshold=21.5 eV[10,14]) meant that there was a significant background signal in the range 11–18 eV caused by parent ion emission being excited by second-order radiation from 22–36 eV. This was particularly unwelcome when making the single-bunch lifetime measurements of the much weaker SiF_3 and SiF_2 emissions induced by photons in the range 12–19 eV in first order. Hence it was impossible to measure these lifetimes without the decay of the signal being dominated by SiF_4^+ $\tilde{D}$-state emission ($\tau = 9.3$ ns[10]).

The lifetime data were analysed using a nonlinear least-squares program, FLUOR,[15] developed by staff at the Daresbury Laboratory. The measured fluorescence signal is not a simple decay, but is a convolution of the fluorescence decay with a ''prompt'' instrument component, plus a background. The prompt component is the average time profile of the single bunch in the storage ring convoluted with the response time of the photomultiplier tube and the associated detection electronics. The signal observed with no gas present, arising from scattering of the synchrotron radiation, offers a reasonable approximation to the prompt component of the measured fluorescence. This ''prompt signal'' was measured prior to the lifetime decays for SiF_4 at BESSY 1. The scattered light was maximized by setting both monochromators to zero order, i.e., $\lambda_1 = \lambda_2 = 0$. A model, either the sum of one or two exponential functions, was chosen to represent the time behavior of the fluorescence. The choice of model depended on whether one or two emissions were being excited at a particular excitation wavelength λ_1, and whether λ_2 was set to zero order or not. The model function could then be convoluted with the prompt signal and fitted to the experimental data by minimizing the Poisson-weighted sum of the squares of the residuals to obtain experimental values of the lifetimes (τ_1, τ_2), amplitudes (A_1, A_2), and the background (B), where

$$y = A_1 \exp(-t/\tau_1) + A_2 \exp(-t/\tau_2) + B.$$

If the decay times are very much longer than the duration of the prompt signal, it is possible to use a model function without this convolution procedure. However, since all the lifetimes of emitting states of SiF_4^+, SiF_3, and SiF_2 are less than ~ 10 ns and the response time of the photomultiplier tube is as long as 1.5 ns, we found it essential to deconvolute the prompt signal from our lifetime data. We believe that this procedure is superior to that we have used in the past to analyze single-bunch lifetime data, where we have simply ignored that part of the decay in the first 3 to 4 ns after the excitation pulse.[10,16] This procedure works satisfactorily for lifetimes greater than ~ 30 ns, but is not appropriate if there are emitters present with lifetimes comparable to the response time of the detection electronics.

TABLE I. Energetics of dissociation channels of SiF_4 and SiF_4^+.

Neutral/parent ion	Dissociation channel	Dissociation energy/eV	Adiabatic (vertical) IP/eV[a]
SiF_4^+ $\tilde{D}\ ^2A_1$			21.55(21.55)
	$SiF_2^+ + F_2$	20.92	
$\tilde{C}\ ^2T_2$			19.30(19.46)
	$SiF\ X\ ^2\Pi + 3F$	18.58	
$\tilde{B}\ ^2E$			18.0[b](18.0)
$\tilde{A}\ ^2T_2$			17.1(17.4)
	$SiF_2\ \tilde{A}\ ^1B_1 + 2F$[c]	17.15	
	$SiF\ X\ ^2\Pi + F_2 + F$	16.98	
	$SiF_3^+ + F$	16.21	
$\tilde{X}\ ^2T_1$			15.8(16.5)
	$SiF_2\ \tilde{A}\ ^1B_1 + F_2$	15.55	
	$SiF_2\ \tilde{a}\ ^3B_1 + 2F$[d]	14.94	
	$SiF_2\ \tilde{a}\ ^3B_1 + F_2$	13.34	
	$SiF_2\ \tilde{X}\ ^1A_1 + 2F$	11.68	
	$SiF_2\ \tilde{X}\ ^1A_1 + F_2$	10.08	
	SiF_3^* (480 nm) + F	$\geqslant 9.76$[e]	
	$SiF_3\ \tilde{X}\ ^2A_2''(?)$[f] + F	7.18	
$SiF_4\ \tilde{X}\ ^1A_1$			0

[a]Reference 14.
[b]References 17 and 18.
[c]Reference 7(a).
[d]Reference 6.
[e]The minimum energy of the SiF_3^*+F channel of 9.76 eV assumes that emission at 480 nm occurs to the ground electronic state of SiF_3. The energy of this channel will be higher if emission occurs to an excited state. The maximum energy of SiF_3^*+F is the threshold for fluorescence at $\lambda > 380$ nm of 12.4 ± 0.1 eV (Sec. V).
[f]Symmetry of the ground electronic state of the CF_3 radical (Ref. 19).

III. THERMOCHEMISTRY OF SiF_4 AND SiF_4^+

The thermochemistry of the valence states of SiF_4^+ and of the dissociation channels of SiF_4 to neutral products is shown in Table I. The electron configuration of the five highest-occupied outer-valence molecular orbitals of SiF_4 is $\cdots(2a_1)^2(2t_2)^6(1e)^4(3t_2)^6(1t_1)^6$, where the numbering scheme only involves those orbitals formed from Si $3s,3p$ and F $2s,2p$ atomic orbitals. Adiabatic ionization potentials (IP) are given in Table I, the data mostly being taken from our recent threshold photoelectron study.[14] There is some doubt about the adiabatic IP to the ground state of the ion because, like all MX_4 molecules, SiF_4 undergoes extensive Jahn–Teller distortion upon ionization such that the Franck–Condon factor at threshold is very small. From studies of charge-transfer reactions of atomic ions with SiF_4, Kickel *et al.*[20] obtained a much lower value for the adiabatic IP of 15.29 ± 0.08 eV. However, this value was not obtained directly (unlike that from photoelectron spectroscopy), but rather from a fit to the variation of reaction cross sections in

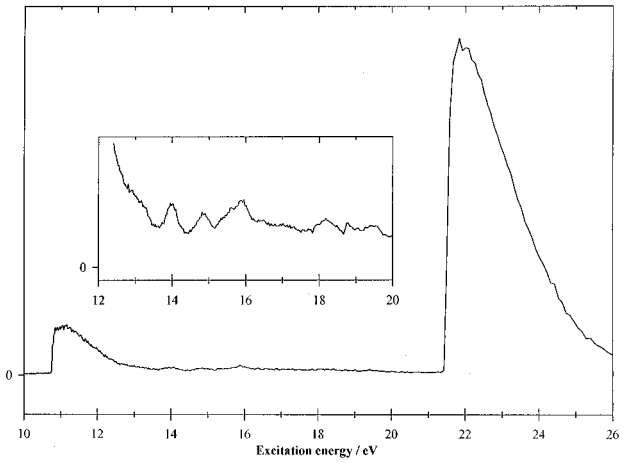

FIG. 1. Fluorescence excitation spectrum of SiF_4 between 10 and 26 eV recorded at the BESSY 1 synchrotron source with an optical resolution of 0.2 nm, equivalent to a resolution of ~0.05 eV at 17 eV. The fluorescence has not been normalized to the vacuum-UV radiation from the primary monochromator.

the threshold region to an empirical model. We therefore prefer to use the value obtained directly from threshold photoelectron spectroscopy. The energies of the neutral dissociation channels of SiF_4 are calculated from the heats of formation of SiF_x ($x=1-4$) and F given by Fisher *et al.*[21] These values come from the same study of charge-transfer reactions of atomic ions with SiF_4 as mentioned above, with values for SiF_2 and SiF_3 being up to 1 eV different from those given in the JANAF tables.[22] The excitation energies of the (0,0) bands of the $\tilde{A}-\tilde{X}$ and $\tilde{a}-\tilde{X}$ transitions in SiF_2 are 5.47 and 3.26 eV, respectively.[6,7] The visible emission spectrum of SiF_3 covering the range 350–850 nm[9] is very poorly characterized. The symmetries of the states involved in the transition are unknown, and it is not even known whether the lower state of this transition is the ground electronic state of the radical. The energy of the SiF_3^*+F channel, spanning the range 9.76–12.4 eV, is discussed in Sec. V.

IV. RESULTS

The fluorescence excitation spectrum of SiF_4 between 10 and 26 eV recorded at BESSY with an optical resolution of 0.2 nm and the secondary monochromator set at zero order is shown in Fig. 1. A very similar spectrum was also obtained at Daresbury. The spectrum is dominated by a nonresonant peak with threshold at 21.5 eV whose shape is characteristic of a photoionization process.[10] This energy corresponds to the adiabatic IP of the $\tilde{D}\ ^2A_1$ excited valence state of SiF_4^+. Fluorescence from this state has been observed in earlier fluorescence excitation studies,[10,11] in coincidence experiments,[14] and in high-resolution emission studies between bound states of SiF_4^+.[23] This process is nonresonant because, as in photoelectron spectroscopy, the ejected electron can carry away the excess energy, and the emission intensity above threshold is governed essentially by the variation of the partial ionization cross section of the emitting state (i.e., $SiF_4^+\tilde{D}\ ^2A_1$) with energy. Thus fluorescence is still observed for photon energies in excess of 10 eV above threshold.[10] This nonresonant peak is also observed in Fig. 1 with a threshold of 10.75 eV, due to second-order radiation from the primary monochromator. Much weaker resonant peaks are observed in the fluorescence excitation spectrum at energies of 13.0, 13.9, 14.8, 15.9_5, 18.1, and 19.5 eV. The peak at 13.0 eV (which in our spectrum appears as a shoulder on the side of the second-order nonresonant peak at 10.75 eV) has been observed previously by Suto *et al.*[11] whereas the other peaks are observed here for the first time in such an experiment. They all have shapes consistent with a photoabsorption rather than a photoionization process, where for each peak the excitation spectrum increases from threshold as the photon energy scans through the Franck–Condon region of the excited (usually Rydberg) state of SiF_4, reaches a maximum, and recedes to the baseline. Note however in the insert to Fig. 1 that the baseline does not correspond to zero signal, but to a background level due to the second-order, nonresonant emission from the $SiF_4^+\tilde{D}$ state. The emitter may either be the excited state itself or a fluorescing fragment formed from its (pre-)dissociation. We show later that the latter process is always occuring.

Dispersed emission spectra between 190 and 450 nm recorded at primary photon energies corresponding to the major peaks in the fluorescence excitation spectrum are shown in Fig. 2. At an energy of 21.8 eV [Fig. 2(d)], emission originates solely from the $\tilde{D}\ ^2A_1$ state of SiF_4^+. The spectrum is dominated by a broad band centered at 310 nm which was first observed by Aarts.[24] This band is assigned to bound-free emission to the repulsive $\tilde{A}\ ^2T_2$ state of the parent ion which dissociates directly to SiF_3^++F.[14] Much weaker peaks centered at ~250 and 380 nm are due to emission to the $\tilde{X}\ ^2T_1$ and $\tilde{B}\ ^2E$ states of SiF_4^+. Transitions to both these states are formally forbidden by optical selection rules. The $\tilde{D}\ ^2A_1-\tilde{C}\ ^2T_2$ band of SiF_4^+ shows discrete rovibrational structure for low vibrational levels of the $\tilde{C}$ state,[23] but its band center at 551 nm is outside the sensitivity range of the dispersive secondary monochromator used here. Note that the difference in the vertical ionization energies of the valence bands of SiF_4^+ predicts emissions at $\sim 250(\tilde{D}-\tilde{X})$, $290(\tilde{D}-\tilde{A})$, $350(\tilde{D}-\tilde{B})$, and $580(\tilde{D}-\tilde{C})$ nm, in good agreement with the experimental values. At an excitation energy of 13.0 eV [Fig. 2(a)] the spectrum is dominated by a band covering approximately the same wavelength range as that of $SiF_4^+\tilde{D}-\tilde{A}$. We assign this band either to $SiF_4^+\tilde{D}-\tilde{A}$ emission produced by second-order radiation at 26.0 eV from the primary monochromator or to SiF_3. Most likely, the signal is due to both processes, although there is some evidence from the lifetime measurements that the former process dominates (Sec. V). Emission is also produced at $\lambda > 450$ nm due to the SiF_3 radical (see below), but the secondary monochromator and photomultiplier tube used in these experiments is insensitive to these longer wavelengths. The dispersed spectra at excitation energies of 13.9 and 14.8 eV are very similar to that in Fig. 2(a), and are not shown. At an energy of 15.9 eV [Fig. 2(b)], in addition to the 280–340 nm band which we assign primarily to $SiF_4^+\tilde{D}-\tilde{A}$ produced by second-order ra-

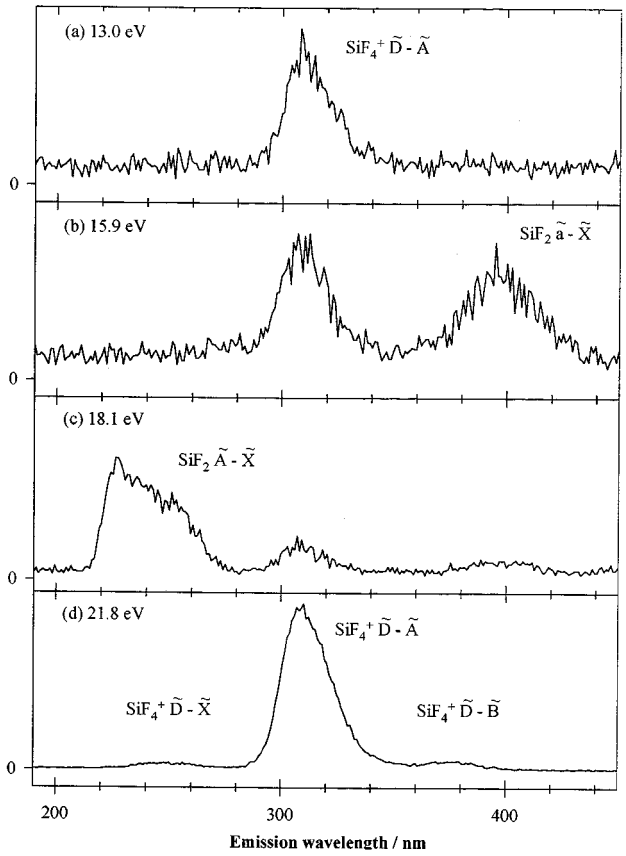

FIG. 2. Dispersed emission spectra for SiF_4 photoexcited at (a) 13.0, (b) 15.9, (c) 18.1, and (d) 21.8 eV. The optical resolution was ~ 4 nm. No attempt has been made to allow for the variation of sensitivity of the detection system with wavelength, but it is predicted to decrease rapidly for $\lambda > 450$ nm. Assignments of the main emission bands are given. Note that for photon energies below 20 eV, the $SiF_4^+\tilde{D}-\tilde{A}$ band arises due to second-order radiation from the primary monochromator.

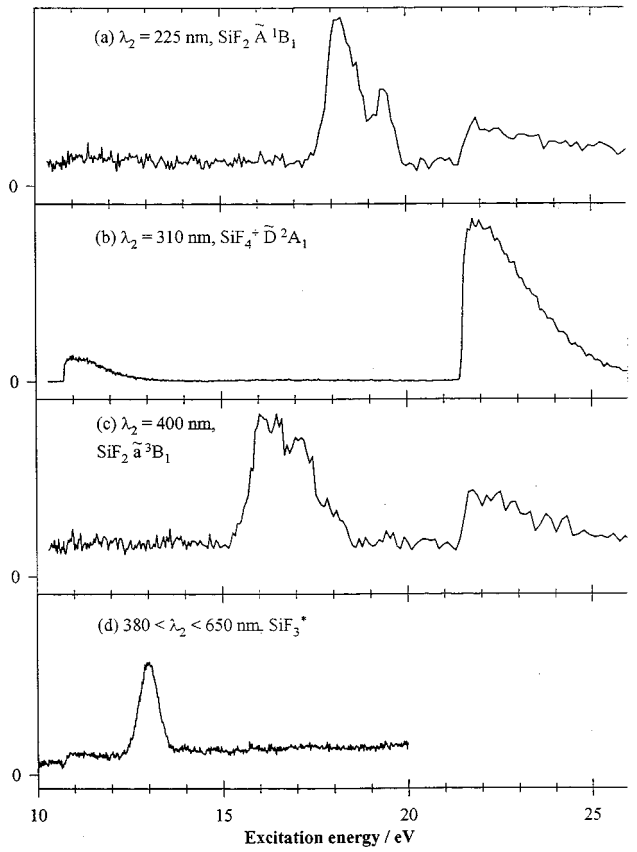

FIG. 3. Action spectra of SiF_4 recorded at the BESSY 1 synchrotron source between 10 and 26 eV with detection of fluorescence at (a) 225 ± 4, (b) 310 ± 4, and (c) 400 ± 4 nm, respectively. These three wavelengths correspond primarily to the peaks of the SiF_2 $\tilde{A}\,^1B_1-\tilde{X}\,^1A_1$, $SiF_4^+\tilde{D}\,^2A_1-\tilde{A}\,^2T_2$, and SiF_2 $\tilde{a}\,^3B_1-\tilde{X}\,^1A_1$ bands. (d) Fluorescence excitation spectrum of SiF_4 recorded at the Daresbury synchrotron source with an EMI 9883 QB photomultiplier tube filtered to detect fluorescence only in the range 380–650 nm. Emission in this range is primarily due to the visible band of SiF_3 (Ref. 9). The optical resolution is 0.2 nm in (a)–(c), 0.1 nm in (d). Fluorescence has not been normalized to the VUV radiation from the primary monochromator in any of the spectra.

diation at 31.8 eV, a new band between 360 and 440 nm is observed. This is the wavelength range where the spin-forbidden transition in SiF_2 from the lowest triplet state, $\tilde{a}\,^3B_1$, to the ground state, $\tilde{X}\,^1A_1$, occurs. This spectrum was first observed in emission with vibrational resolution by Rao[25] who confirmed that the lower state was indeed the ground electronic state, and very recently has been partially rotationally analyzed in a laser-induced phosphorescence study by Karolczak *et al.*[6] At an excitation energy of 18.1 eV [Fig. 2(c)], in addition to the 290–340 nm band which is now very weak, a new UV band between 220 and 280 nm is observed, in exact agreement with the range of wavelengths over which the SiF_2 $\tilde{A}\,^1B_1-\tilde{X}\,^1A_1$ transition occurs.[2,4,5,7]

Figures 3(a)–3(c) show three action spectra where the primary monochromator is scanned for detection of fluorescence at a specific wavelength, $\lambda_2\pm4$ nm. The values of λ_2 were determined by choosing suitable peaks from the dispersed emission spectra (Fig. 2). Thus, action spectra were recorded at $\lambda_2=225$ nm corresponding to the peak of SiF_2 $\tilde{A}-\tilde{X}$ emission, 310 nm corresponding to $SiF_4^+\tilde{D}-\tilde{A}$ emission, and 400 nm corresponding to SiF_2 $\tilde{a}-\tilde{X}$ emission. Not surprisingly, the action spectrum at 310 nm [Fig. 3(b)] almost mimics the excitation spectrum (Fig. 1 where $\lambda_2=0$) since $SiF_4^+\tilde{D}-\tilde{A}$ emission is the most intense band in the excitation range 10–26 eV. Action spectra at 225 and 400 nm are dominated by broad bands peaking at 18.1 and 15.9 eV with thresholds at 17.4 ± 0.2 and 15.2 ± 0.2 eV. In the ranges 17–20 eV and 15–18 eV emission is mainly observed from the $\tilde{A}\,^1B_1$ and $\tilde{a}\,^3B_1$ states of SiF_2, respectively. The weak peak in both Figs. 3(a) and 3(c) with a threshold at 21.5 eV is due to emission from the $\tilde{D}\,^2A_1$ state of SiF_4^+ which still has weak remnants at 225 nm (due to $SiF_4^+\tilde{D}-\tilde{X}$) and 400 nm ($SiF_4^+\tilde{D}-\tilde{B}$). Figure 3(d) shows the excitation spectrum between 10 and 20 eV recorded at Daresbury with a resolution of 0.1 nm with detection of undispersed fluorescence through a visible cut-on filter (Schott LF 399). The effective range of wavelengths over which emission is observed in this experiment is then $\sim 380-650$ nm, and as such this constitutes a very low-resolution action spectrum. It can clearly be seen that the peak at 13.0 eV in the excitation spectrum gives rise pre-

TABLE II. Lifetimes of emission bands observed from VUV excitation of SiF_4 in the range 10–26 eV.

E_1 /eV	λ_2 /nm (±50 nm)	τ_n /ns	A_n	Reduced χ^2	Emitter(s)
13.0	0	3.0±0.8	1.0±0.5	2.42	SiF_3^*, $SiF_4^+\tilde{D}\ ^2A_1$
		9.6±1.0	0.8±0.3		
13.0	310	9.3±0.3		0.97	$SiF_4^+\tilde{D}\ ^2A_1$
13.0	480	3.9±0.7		1.71	SiF_3^*
15.9	0	2.6±0.4	1.0±0.1	1.29	$SiF_2\ \tilde{a}\ ^3B_1$, $SiF_4^+\tilde{D}\ ^2A_1$
		10.6±1.4	0.4±0.1		
18.1	0	11.0±1.0		1.78	$SiF_2\ \tilde{A}\ ^1B_1$, $SiF_4^+\tilde{D}\ ^2A_1$
18.1	225	11.2±1.5		2.01	$SiF_2\ \tilde{A}\ ^1B_1$
21.8	310	9.16±0.02		1.33	$SiF_4^+\tilde{D}\ ^2A_1$

dominantly to visible emission, as has been observed by Suto *et al.*[9] with fixed-energy discharge lamp sources. We show later that this emission is due to the SiF_3 radical. From Fig. 3(d) we also determine the threshold for production of SiF_3^* to be 12.4±0.1 eV.

Lifetimes of the emissions induced in SiF_4 at excitation energies of 13.0, 15.9, 18.1, and 21.8 eV were measured using the single-bunch mode of the BESSY source. As mentioned in Sec. II, these experiments used a fast Hamamatsu R6060 photomultiplier tube and a secondary monochromator (JY H20VIS) with a grating blazed at a longer wavelength than that used in the multibunch experiments. Both factors increased the sensitivity range of the secondary monochromator in the visible region, and for the first time made the observation of emission in SiF_3 at $\lambda > 400$ nm possible at BESSY 1. Resolution of both monochromators was degraded to increase flux. In nearly all cases lifetimes were recorded both with the secondary monochromator set to zero order and to the wavelength(s) at which the emission spectrum maximizes. Typical accumulation times were 30–120 min per decay. The lifetimes were analyzed both by single- and double-exponential functions, with deconvolution of the prompt signal (no gas, $\lambda_1 = \lambda_2 = 0$) as described in Sec. II. In choosing the best fit, consideration was given to minimize the reduced chi-squared values, to minimize the pairwise correlation functions of the fitted parameters, and to ensure both that the residuals of the fit showed nonsystematic trends and that the fitted background agreed with its experimental value. The results of the best fits are shown in Table II, and typical decays from SiF_4 excited at 13.0 eV with $\lambda_2 = 0$, 310 and 480 nm are shown in Figs. 4(a)–4(c), respectively.

V. DISCUSSION

First we consider the assignment of the peaks in the fluorescence excitation spectrum (Fig. 1). Since the three highest occupied molecular orbitals of SiF_4 (i.e., $1t_1$, $3t_2$, and $1e$) are essentially nonbonding orbitals located on the fluorine atoms,[26] the lowest principal quantum number for Rydberg states originating from these orbitals is expected to be $n = 3$. The next two highest orbitals, $2t_2$ and $2a_1$, are essentially Si–F σ bonding in character,[26] and therefore the lowest principal quantum number for Rydberg states derived from these orbitals is $n = 4$. The peaks we observe at 13.0, 14.8, and 15.9 eV are observed in absorption,[11] albeit with very different intensity ratios. These three peaks and the peaks at 13.9 and 19.5 eV are also observed by electron energy loss spectroscopy (EELS),[27] although the latter two peaks are observed at slightly different energies of 13.75 and

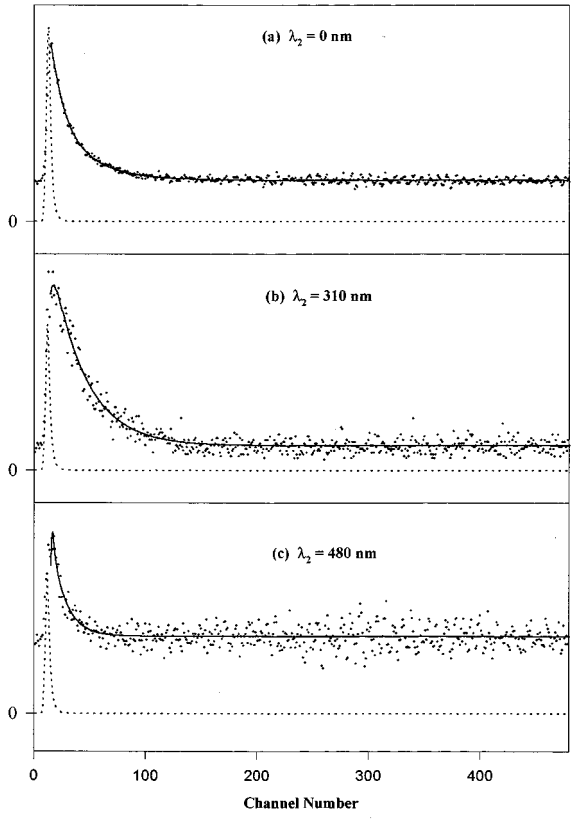

FIG. 4. Decay of the fluorescence following excitation of SiF_4 at 13.0 eV with single-bunch, pulsed radiation from the BESSY 1 synchrotron source. The secondary monochromator is set to (a) $\lambda_2 = 0$, (b) $\lambda_2 = 310$, and (c) $\lambda_2 = 480$ nm, respectively. Each spectrum shows the experimental data points, the prompt signal (dashed line), and the fit to the data (solid line) using the method described in Sec. II. The time calibration is 0.3125 ns per channel. In (a), emission is due to SiF_3^* and $SiF_4^+\tilde{D}\ ^2A_1$, and the decay fits best to a bi-exponential function with $\tau_1 = 3.0 \pm 0.8$ and $\tau_2 = 9.6 \pm 1.0$ ns with approximately equal amplitudes ($A_1 \approx A_2$). In (b), emission is only due to $SiF_4^+\tilde{D}\ ^2A_1$, and the decay fits best to a single exponential function with $\tau = 9.3 \pm 0.3$ ns. In (c), emission is only due to SiF_3^*, and again the decay fits best to a single exponential function with $\tau = 3.9 \pm 0.7$ ns.

TABLE III. Peak positions and assignments from fluorescence excitation spectroscopy of the Rydberg and ionic states of SiF_4 in the range 10–26 eV that lead to fluorescence, and assignments of the fluorescing fragments/ions and their lifetimes.

E/eV[a]	Assignment	(IP-E)/eV	$(n-\delta)$	δ[b]	Emission range/nm	Emitter	Lifetime/ns
13.0	$(1t_1)^{-1}3p$	3.5	1.97	1.03	~380–800	SiF_3^*	3.9±0.7
	or $(3t_2)^{-1}3s$	4.4	1.76	1.24			
13.9	$(3t_2)^{-1}3p$	3.5	1.97	1.03	~380–800	SiF_3^*	3.9±0.7
14.8	$(1t_1)^{-1}3d$	1.7	2.83	0.17	~380–800	SiF_3^*	3.9±0.7
	or $(1e)^{-1}3p$	3.2	2.06	0.94			
15.95	$(3t_2)^{-1}3d$	1.45	3.06	−0.06	~360–440	$SiF_2\ \tilde{a}\ ^3B_1$	2.6±0.4[c]
	or $(3t_2)^{-1}4p$	1.45	3.06	0.94			
18.1	$(2t_2)^{-1}4p$	1.36	3.16	0.84	~220–280	$SiF_2\ \tilde{A}\ ^1B_1$	11.2±1.5
19.45	$(2a_1)^{-1}4s$	2.1	2.54	1.46	~220–280	$SiF_2\ \tilde{A}\ ^1B_1$	11.2±1.5
21.5[d]	$(2a_1)^{-1}\rightarrow SiF_4^+\ D\ ^2A_1$				~280–350	$SiF_4^+\tilde{D}\ ^2A_1$	9.16±0.02

[a]Effects of second-order radiation producing $SiF_4^+\tilde{D}$-state emission at excitation energies less than 21.5 eV are ignored in this Table.

[b]Quantum defect, δ, defined by the equation $E=\text{IP-}[R_H/(n-\delta)^2]$, where R_H is the Rydberg constant and n is the principal quantum number of the Rydberg orbital. Calculated using the appropriate vertical ionization potentials for SiF_4 from threshold photoelectron spectroscopy (Ref. 14).

[c]It is unclear whether this is the lifetime of fluorescence or of intersystem crossing (see the text).

[d]Threshold for fluorescence, not peak position.

19.65 eV in that study. The peak at 18.1 eV is not observed by these other two complementary techniques. We comment, however, that only those Rydberg states of SiF_4 which dissociate to a fluorescing excited state of a fragment of SiF_4 are observed in our experiment, whereas both absorption and EELS may be used to observe all the Rydberg states whose transitions from the ground state are allowed by optical selection rules. Furthermore, both spin and orbital selection rules are not particularly strict in EELS, especially at high scattering angles, so that many more peaks are observed than in the absorption spectrum over the same region.[27] Using approximate values for the predicted quantum defects of ns, np, and nd Rydberg orbitals centered on F(Si) atoms of $\delta=1.20(1.80)$, 0.75(1.36), and 0.0(0.10),[28] respectively, and vertical IPs for the five valence orbitals of SiF_4 given in Table I, we can make assignments of the peaks in the fluorescence excitation spectrum (Table III). Due to the low resolution of the spectrum and the uncertainty in the ionization thresholds to which the possible Rydberg series converge, they do not represent a unique set of assignments, and there are blends. However, with the exception of the transition to the $(2a_1)^{-1}4s$ Rydberg state at 19.5 eV, transitions to all the other states from the ground state of SiF_4 are optically allowed.

The nature of the emitters of the fluorescence induced in the excitation range 10–25 eV is now discussed. First, we consider the emission excited at 13.0 eV. Figure 3(d) shows that emission over the excitation range 12.4–13.6 eV occurs in the visible region with wavelengths in the range ~380–650 nm. In theory, the emitter could be the parent molecule, SiF_4, or a fragment. However, the evidence both from absorption and electron energy loss spectroscopy is that SiF_4 is transparent in the vacuum-UV below 11 eV, and no valence states of the molecule exist ~2 to 3 eV below the excitation energy of 13.0 eV. Therefore, emission in the parent molecule can be discounted. The strongest reasons for assigning the emission to the SiF_3 radical are not spectroscopic, but thermodynamic. The ground state of SiF_3+F is calculated to occur at 7.18 eV, so emission in the visible region is energetically possible for an excitation energy of 13.0 eV. The ground states of $SiF_2(\tilde{X}\ ^1A_1)$ and $SiF(X\ ^2\Pi)$ lie higher in energy at 10.08 and 16.98 eV, and SiF emission can therefore be discounted immediately. The lowest excited state of SiF_2, the $\tilde{a}\ ^3B_1$ state, lies 3.26 eV above the ground state,[6] so the threshold energy to produce $SiF_2\ \tilde{a}\ ^3B_1$ is 13.34 eV, above the experimentally-determined threshold of 12.4 ±0.1 eV. Data on the electronic spectroscopy of SiF_3 is scarce, and no microwave nor infrared spectrum of this radical in its ground electronic state in the gas phase have been reported. The first assignment of any emission to SiF_3, that obtained in the region 210–260 nm by Wang *et al.*[29] by passing SiF_4 through a microwave discharge, has subsequently been shown to be incorrect, and all the observed bands are due to $SiF_2\ \tilde{A}-\tilde{X}$. There have been two observations of a broad, visible emission band ($\lambda_{peak}=632$ nm, FWHM=240 nm) from the reaction of fluorine atoms produced in a discharge flow system with single-crystal silicon samples.[1,2] Both studies have assigned this emission to the SiF_3 radical. However, this assignment has been made more on the basis that the emission is *not* due to any known band system in SiF_2 or SiF, than due to a detailed knowledge of the spectroscopy of SiF_3. The problem with all these experimental techniques is that the excitation energy is not controlled. The only previous study using vacuum-UV photon excitation prior to our work is that of Suto *et al.* They dispersed the emission induced from both SiF_4[9] and SiF_3H[3] excited with fixed-energy discharge lamp line sources between 90 and 100 nm. The emission from the lamp was passed through a 1 m VUV monochromator before impacting on the sample. In both cases, two bands were observed by a red-sensitive (190–800 nm), cooled photomultiplier tube—one between

290 and 340 nm, and another much broader band between 350 and 800 nm. Although the former band covers almost an identical region to the $SiF_4^+\tilde{D}-\tilde{A}$ band, second-order radiation cannot be the cause since the emission source is not continuous. They assigned both bands to the SiF_3 radical, and commented that the spectra were similar to that in CF_3 where a discrete UV band (between 200 and 300 nm) and a broad visible band (between 400 and 800 nm) are known to exist.[30]

While the assignments of the spectra in CF_3 have been supported by *ab initio* calculations,[19] there have been no calculations on the energies of excited states of the SiF_3 radical. It seems clear that the emission we observe in Fig. 3(d) at $\lambda > 380$ nm is the same broad visible band between 350 and 800 nm observed by Suto *et al.*,[3,9] and is probably the same emission as that observed in the plasma-simulated experiments peaking at 632 nm.[1,2] What is not clear is whether this emission occurs to the ground state or to an excited state of the radical. The large width of the band suggests that emission occurs to an excited state of SiF_3 which is repulsive in the Franck–Condon region, a situation similar to that in CF_3.[19] If this is the case, we can calculate an upper limit to the energy of this lower state relative to the ground state of SiF_3. We have measured the lifetime of this emission with the secondary monochromator, λ_2, set at 480 ± 50 nm near to the peak of the emission spectrum,[9] corresponding to a photon energy of 2.58 ± 0.25 eV. The minimum energy of the emitting state in SiF_3 is then 9.76 eV (Table I), so for this emission to be observed at a threshold energy of 12.4 eV the excited state of SiF_3 to which emission occurs must lie less than ~ 2.6 eV above the ground state. Note that the *ab initio* calculations on CF_3 predict that the lower state of its visible band lies ~ 4 eV above the ground state.[19] There is also some evidence that the ground state of SiF_3 is bound, in that its lifetime is long enough for electron-impact ionisation cross-section measurements to be made on the radical in a charge-transfer experiment.[31]

The UV band between 290 and 340 nm, which was observed by Suto *et al.* from photodissociation of SiF_4 at 13.0 eV [Fig. 1(b) of Ref. 9] and assigned to a different emission in the SiF_3 radical, covers an almost identical range to the $SiF_4^+\tilde{D}-\tilde{A}$ band. Two factors suggest that the former emission dominates in their spectrum while the latter produced by second-order radiation from the excitation source is dominant in ours. First, whilst our excitation source is monochromatised continuous radiation from a synchrotron, theirs uses line sources from a capillary discharge lamp. Therefore, while second-order radiation will be a problem in our experiment, as we have observed before,[12] it seems highly unlikely to be the case in theirs. Second, we have measured the lifetime of the emission(s) excited at 13.0 eV with λ_2 set to zero order, to 310, and to 480 nm (Table II). With $\lambda_2 = 0$ the decay fits best to a double exponential of approximately equal amplitudes ($A_1 \approx A_2$) with $\tau_1 = 3.0 \pm 0.8$ and $\tau_2 = 9.6 \pm 1.0$ ns, implying that two emitters are present. With $\lambda_2 = 310 \pm 50$ nm and hence isolating the UV emission, a single exponential decay is observed with $\tau = 9.3 \pm 0.3$ ns. This value is in excellent agreement both with that obtained previously[10] and with that obtained in this work (9.16 ± 0.02 ns) when SiF_4 was excited at 21.8 eV into the $\tilde{D}\ ^2A_1$ state ionic continuum (Table II). With $\lambda_2 = 480 \pm 50$ nm, a single exponential decay is also obtained with $\tau = 3.9 \pm 0.7$ ns. This value of λ_2 was chosen as a compromize to maximize the SiF_3 visible emission while minimizing emission from the $SiF_4^+\tilde{D}\ ^2A_1$ state.[9,24] We conclude that the lifetime of the electronic state of SiF_3 giving rise to the visible emission band is 3.9 ns, and that in our experiment the band observed simultaneously between 290 and 340 nm is predominantly due to emission from the $SiF_4^+\tilde{D}\ ^2A_1$ state produced in second order, and not due to another emitting state of SiF_3. It is worth noting, however, that Suto *et al.*[9] found that the relative intensity of the SiF_3 UV band compared to that of the visible band changed with excitation energy, implying that the two emissions have different upper states. It is possible, therefore, that the lifetime of the electronic state giving rise to SiF_3 UV emission coincidentally has the same value as that of the $SiF_4^+\tilde{D}\ ^2A_1$ state. On balance we believe this to be unlikely. It is clear, however, that high quality *ab initio* calculations are needed on the spectroscopic and dynamical properties of excited electronic states of SiF_3, and it is hoped that this work will stimulate such studies.

We now consider the emission from SiF_4 excited at 15.9 eV. In addition to the 290–340 nm band, a new band between 360 and 440 nm is observed. This band is assigned to the $\tilde{a}\ ^3B_1-\tilde{X}\ ^1A_1$ spin-forbidden transition in SiF_2. First observed in emission at vibrational resolution by Rao,[25] the origin band of this electronic transition has now been observed with almost complete rotational resolution.[6] The rotational analysis has determined the geometry of the $\tilde{a}\ ^3B_1$ state to be $r(\mathrm{Si–F}) = 1.586$ Å and $\vartheta(\mathrm{FSiF}) = 113.1°$, compared with ground state values from microwave spectroscopy of 1.591 Å and 101.0°, respectively.[32] The intensity distribution of the rotational branches in the laser-induced phosphorescence spectrum suggest that the triplet–singlet transition gains oscillator strength primarily by spin–orbit coupling of the $\tilde{a}\ ^3B_1$ state with higher-lying singlet states of B_2 symmetry. The lowest such state in SiF_2 is the valence state at 161 nm,[33] 4.44 eV above the $\tilde{a}\ ^3B_1$ state. There have been no experimental determinations of the lifetimes of either state, although a recent *ab initio* study has calculated the lifetime of this $\tilde{B}\ ^1B_2$ state to be 11.5 ns.[8] We have measured the lifetime of the emissions excited at 15.9 eV with λ_2 set to zero order (Table II). Unfortunately, measurements were not made at $\lambda_2 = 400$ nm, isolating the SiF_2 $\tilde{a}–\tilde{X}$ emission. A double-exponential decay is obtained with $\tau_1 = 2.6 \pm 0.4$ and $\tau_2 = 10.6 \pm 1.4$ ns, the shorter lifetime component having over twice the amplitude of the longer. The 10.6 ns component is probably due to the $SiF_4^+\tilde{D}\ ^2A_1$ state, and it therefore suggests that the lifetime of the SiF_2 $\tilde{a}\ ^3B_1$ state is 2.6 ns. This is an exceptionally small value for a metastable state, and could only result if the spin–orbit coupling with $^1B_2$ states is so strong that it is inappropriate to describe the $\tilde{a}\ ^3B_1$ state as a triplet. The other possibility is that the life-

time of the $\tilde{a}\,^3B_1$ state is much longer than can be measured with a pulsed source with only 208 ns between pulses, i.e., $\tau > \sim 200$ ns, but this leaves unanswered the question of what is the cause of the 2.6 ns component in the decay. Karolczak *et al.*[6] observed a sudden decrease in intensity in their laser-induced phosphorescence study for vibrational levels $\nu_2' > 2$. They speculated that a rapid nonradiative decay channel (e.g., intersystem crossing to the ground state) turns on at these excited state vibrational energies, and it is just possible that this process is the cause of the 2.6 ns component.[34] Obviously lifetime measurements as a function of vibrational state of $\tilde{a}\,^3B_1$ are needed to confirm this theory, whereas our experiment only gives a value of the lifetime for the range of vibrational levels of $\tilde{a}\,^3B_1$ populated by photodissociation of SiF_4^*. Our experiment also gives no information on whether the other product of the photodissociation is F_2 or F+F. Both channels are energetically possible (Table I); the threshold for production of $SiF_2\ \tilde{a}\,^3B_1$, 15.2 ± 0.2 eV, lies ~ 0.3 eV above the dissociation energy to $SiF_2\ \tilde{a}\,^3B_1 + 2F$, and 1.9 eV above that to $SiF_2\ \tilde{a}\,^3B_1 + F_2$. Direct dissociation of the $(3t_2)^{-1}3d/(3t_2)^{-1}4p$ singlet Rydberg state(s) of SiF_4 to $SiF_2\ \tilde{a}\,^3B_1 + F_2\ X\,^1\Sigma_g^+$ is formally spin forbidden, although if the $\tilde{a}\,^3B_1$ state acquires substantial singlet character through spin–orbit mixing this selection rule is relaxed. Conversely, if photodissociation occurs sequentially in two steps $[SiF_4^* \rightarrow SiF_3^* + F(^2P) \rightarrow SiF_2\ \tilde{a}\,^3B_1 + F(^2P) + F(^2P)]$ via an excited electronic state of SiF_3 with doublet symmetry, these processes are both spin allowed. It is worth noting that there is little change in the FSiF bond angle between SiF_4^* (109.5° if this state has tetrahedral symmetry) and $SiF_2\ \tilde{a}\,^3B_1$ (113.1°), so if photodissociation is direct there should be little vibrational energy in the $SiF_2\ \tilde{a}\,^3B_1$ state. There has been no experimental determination of the bond angle in SiF_3 in either its ground or in any of its excited states, although it would be surprising if the ground state were not pyramidal and the Rydberg states planar, as in the CF_3 radical.[19]

Finally we consider the emission from SiF_4 excited at 18.1 eV. There are still weak emissions between 290–340 nm and that due to $SiF_2\ \tilde{a}–\tilde{X}$, but the main emission occurs as a new band between 220 and 280 nm. This band is assigned to the $\tilde{A}\,^1B_1–\tilde{X}\,^1A_1$ transition is SiF_2. The origin band was rotationally analyzed by Dixon and Halle,[4] and the geometry of the $\tilde{A}\,^1B_1$ state determined to be $r(\mathrm{Si–F}) = 1.601$ Å and $\vartheta(\mathrm{FSiF}) = 115.9°$. Since both this and the $\tilde{a}\,^3B_1$ state arise primarily from the same orbital configuration $\cdots\ (8a_1)^1(3b_1)^1$,[8,35] both these values are similar to those of the $\tilde{a}\,^3B_1$ state. There has been only one report of an approximate lifetime of the $\tilde{A}\,^1B_1$ state of SiF_2 from a laser-induced fluorescence study of the $\tilde{A}–\tilde{X}$ transition, where an upper limit of 20 ns was determined.[2] We have measured the lifetime of the emissions excited at 18.1 eV with λ_2 set to zero and to 230 ± 50 nm, the peak of the $SiF_2\ \tilde{A}–\tilde{X}$ spectrum (Table II). In both cases a single exponential decay is observed with $\tau = 11.0 \pm 1.0$ and 11.2 ± 1.5 ns, respectively. Since $SiF_2\ \tilde{A}–\tilde{X}$ emission dominates the spectrum at this excitation energy [Fig. 2(c)], it is not surprising that the decays fit to single exponentials at these two values of λ_2 and we determine the lifetime of the $\tilde{A}\,^1B_1$ state of SiF_2 to be 11.2 ± 1.5 ns, confirming the result of Vanhaelemeersch *et al.*[2] Our result is also in good agreement with an *ab initio* calculation of the oscillator strength of the $\tilde{A}–\tilde{X}$ transition in SiF_2, which leads to a calculated lifetime of the $\tilde{A}\,^1B_1$ state of 5.2 ns.[8] Note that even if $SiF_4^+\tilde{D}–\tilde{A}$ emission makes a small contribution to the experimental decay, the lifetime of the upper state (9.16 ns) is too close to that of the major emitter (11.2 ns) for the decay to distinguish double- from single-exponential behavior. Again, our experiment gives no information on whether the other product of the photodissociation of the $(2t_2)^{-1}4p$ Rydberg state is F_2 or 2F. As with the $\tilde{a}\,^3B_1$ state of SiF_2 (see above), the experimental threshold for production of $SiF_2\ \tilde{A}\,^1B_1$, 17.4 ± 0.2 eV, lies ~ 0.3 eV above the dissociation energy to this state with two fluorine atoms, 1.9 eV above the dissociation energy to $SiF_2\ \tilde{A}\,^1B_1 + F_2$. Both direct and sequential photodissociation processes are now spin allowed. The fact that experimental thresholds to both $SiF_2\ \tilde{A}\,^1B_1$ and $\tilde{a}\,^3B_1$ lie close to the thermochemical energy of $SiF_2(\tilde{A}$ or $\tilde{a}) + 2F$ suggests that both photodissociations are probably sequential, proceeding via an excited state of SiF_3.

VI. CONCLUSIONS

We have shown that dispersed emission and, to a lesser extent, action spectroscopy are powerful techniques to determine the nature of the emitter(s) from VUV photoexcitation of SiF_4 into its Rydberg states and the ionization continuum. Combined with tunable radiation from a synchrotron source, we have considerably extended both our earlier measurements made on SiF_4 at energies above 20 eV,[10] and the work of Suto *et al.*[9,11] who only used three line sources in the energy range 12.4–13.8 eV (90–100 nm) for dispersed fluorescence measurements. In general, the results for primary photon energies in the range 12–20 eV follow similar patterns to those observed recently for CF_4.[36] Excitation of Rydberg states in the range 13–15 eV gives rise to SiF_3 emission, in the range 15.5–18.0 eV to $\tilde{a}\,^3B_1–\tilde{X}\,^1A_1$ emission in SiF_2, and in the range 17–20 eV to $\tilde{A}\,^1B_1–\tilde{X}\,^1A_1$ emission in SiF_2. (For CF_4, CF_3 emission is observed in the excitation energy range 13–14 eV, $CF_2\ \tilde{A}\,^1B_1–\tilde{X}\,^1A_1$ emission in the range 15–16 eV. The $\tilde{a}\,^3B_1$ state of CF_2 was not observed in the CF_4 experiments, presumably because the $\tilde{a}–\tilde{X}$ transition is so weak.[37]) Unlike similar studies we have performed on BCl_3 and BBr_3,[12,16] there is only limited similarity between the VUV absorption spectrum and the fluorescence excitation spectrum of SiF_4, suggesting that photodissociation of Rydberg states to fluorescing states of neutral fragments is not a major decay channel. Note also that our experiments give no values of quantum yields for production of these excited states of SiF_2 and SiF_3. Parent ion emission from the $\tilde{D}\,^2A_1$ state of SiF_4^+ is observed for photon energies in excess of the threshold of 21.5 eV. Because emission from this primary photoionisation product is non-resonant and oc-

curs for photon energies well in excess of threshold,[10] emission from this state is also observed at energies below threshold due to the presence of second-order radiation from the 1.5 m primary monochromator. Purely coincidentally, the strongest emission band in $SiF_4^+(\tilde{D}\ ^2A_1-\tilde{A}\ ^2T_2)$ covers a similar range of wavelengths to the UV band in SiF_3 observed by Suto *et al.*[9] Therefore it is not possible to say with total confidence whether the emission between 290 and 340 nm [Figs. 2(a)–2(c)] produced with photon energies <20 eV is due to SiF_4^+ or to SiF_3. Using the single-bunch mode of the synchrotron, lifetimes of all the emitting states have been measured. We have used a new fitting procedure which allowed us to deconvolute the prompt signal from the experimental decays. It was now possible to measure lifetimes less than ~ 5 ns for the first time. The ability to define the wavelength of the emission with the secondary monochromator when more than one emitter was excited at a particular VUV primary energy was particularly important, and meant that the lifetimes of these emissions in SiF_3 and SiF_2 could be measured without the presence of signal from the $SiF_4^+\tilde{D}\ ^2A_1$ state produced in second order. The lifetime of the emitting state in SiF_3 that gives rise to the visible band between 350–800 nm is 3.9 ± 0.7 ns, that of the $\tilde{A}\ ^1B_1$ state of SiF_2 11.2 ± 1.5 ns. The decay from the $\tilde{a}\ ^3B_1$ state of SiF_2 has a component of 2.6 ± 0.4 ns. This value could either be the phosphorescence lifetime of the triplet state, or more likely the lifetime for intersystem crossing of its higher vibrational levels into the ground state. Above all, this work has highlighted the need for high quality *ab initio* calculations on the spectroscopic and dynamic properties of the ground and excited electronic states of the SiF_3 radical.

ACKNOWLEDGMENTS

We thank EPSRC and the Daresbury Laboratory for a Research Grant, a Research Fellowship (DMS), Research Studentships (K.J.B., D.P.S., K.R.Y.) and a CASE award (K.J.B.). H.B. thanks the Deutsche Forschungsgemeinschaft for a PostDoctoral Fellowship. The EU Human Capitol and Mobility programme (contract number CHGE-CT93-0027) and the British Council (ARC bilateral programme with Germany, contract number 326) are also acknowledged for funding. We thank Dr. M. A. Hayes of the Daresbury Laboratory for programming and advice with the use of the lifetime fitting programme FLUOR. Finally, we thank Professor L. C. Lee and Professor D. J. Clouthier for helpful suggestions on different aspects of this work.

[1] V. M. Donnelly and D. L. Flamm, J. Appl. Phys. **51**, 5273 (1980).
[2] S. Vanhaelemeersch, J. van Hoeymissen, D. Vermeylen, and J. Peeters, J. Appl. Phys. **70**, 3892 (1991).
[3] M. J. Mitchell, M. Suto, L. C. Lee, and T. J. Chuang, J. Vac. Sci. Technol. B **5**, 1444 (1987).
[4] R. N. Dixon and M. Halle, J. Mol. Spectrosc. **36**, 192 (1970).
[5] See e.g., J. W. C. Johns, G. H. Chantry, and R. F. Barrow, Trans. Faraday Soc. **54**, 1589 (1958).
[6] J. Karolczak, R. H. Judge and D. J. Clouthier, J. Am. Chem. Soc. **117**, 9523 (1995).
[7] (a) R. D. Johnson, J. W. Hudgens and M. N. R. Ashfold, Chem. Phys. Lett. **261**, 474 (1996); (b) J. S. Horwitz, C. S. Dulcey, and M. C. Lin, *ibid*. **150**, 165 (1988).
[8] See e.g., Z. L. Cai and J. L. Bai, Chem. Phys. **178**, 215 (1993).
[9] M. Suto, J. C. Han, L. C. Lee, and T. J. Chuang, J. Chem. Phys. **90**, 2834 (1989).
[10] I. R. Lambert, S. M. Mason, R. P. Tuckett, and A. Hopkirk, J. Chem. Phys. **89**, 2683 (1988).
[11] M. Suto, X. Wang, L. C. Lee, and T. J. Chuang, J. Chem. Phys. **86**, 1152 (1987).
[12] H. Biehl, J. C. Creasey, D. M. Smith, R. P. Tuckett, K. R. Yoxall, H. Baumgärtel, H. W. Jochims, and U. Rokland, J. Chem. Soc. Faraday Trans. **91**, 3073 (1995).
[13] K. P. Huber and G. Herzberg, *Molecular Spectra and Molecular Structure* (Van Nostrand, New York, 1979), Vol. 4.
[14] D. M. Smith, R. P. Tuckett, K. R. Yoxall, K. Codling, P. A. Hatherly, J. F. M. Aarts, and M. Stankiewicz, J. Chem. Phys. **101**, 10559 (1994).
[15] C. M. Gregory, M. A. Hayes, G. R. Jones, and E. Pantos, Technical memorandum, Daresbury Laboratory, reference DL/SCI/TM98E (1994).
[16] H. Biehl, D. M. Smith, R. P. Tuckett, K. R. Yoxall, H. Baumgärtel, H. W. Jochims, and U. Rokland, Mol. Phys. **87**, 1199 (1996).
[17] D. R. Lloyd and P. J. Roberts, J. Electron Spectrosc. **7**, 325 (1975).
[18] R. Jadnry, L. Karlsson, L. Mattsson, and K. Siegbahn, Chem. Phys. Lett. **49**, 203 (1977).
[19] N. Washida, M. Suto, S. Nagase, U. Nagashima, and K. Morokuma, J. Chem. Phys. **78**, 1025 (1983).
[20] B. L. Kickel, E. R. Fisher, and P. B. Armentrout, J. Phys. Chem. **97**, 10198 (1993).
[21] E. R. Fisher, B. L. Kickel, and P. B. Armentrout, J. Phys. Chem. **97**, 10204 (1993).
[22] M. W. Chase, C. A. Davies, J. R. Downey, D. J. Frurip, R. A. MacDonald, and A. N. Syverud, J. Phys. Chem. Ref. Data **14**, supplement (1985).
[23] S. M. Mason and R. P. Tuckett, Mol. Phys. **60**, 771 (1987).
[24] J. F. M. Aarts, Chem. Phys. **101**, 105 (1986).
[25] D. R. Rao, J. Mol. Spectrosc. **34**, 284 (1970).
[26] R. N. Dixon and R. P. Tuckett, Chem. Phys. Lett. **140**, 553 (1987).
[27] K. Kuroki, D. Spence, and M. A. Dillon, J. Electron. Spectrosc. Relat. Phenom. **70**, 151 (1994).
[28] C. E. Theodosiou, M. Inokuti, and S. T. Manson, At. Data Nucl. Data Tables **35**, 473 (1986).
[29] J. L. F. Wang, C. N. Krishnan, and J. L. Margrave, J. Mol. Spectrosc. **48**, 346 (1973).
[30] M. Suto and N. Washida, J. Chem. Phys. **78**, 1007 (1983).
[31] T. R. Hayes, R. J. Shul, F. A. Baiocchi, R. C. Wetzel, and R. S. Freund, J. Chem. Phys. **89**, 4035 (1988).
[32] V. M. Rao, R. F. Curl, P. L. Timms, and J. L. Margrave, J. Chem. Phys. **43**, 2557 (1965).
[33] J. L. Gole, R. H. Hague, J. L. Margrave, and J. W. Hastie, J. Mol. Spectrosc. **43**, 441 (1972).
[34] D. J. Clouthier (private communication).
[35] A. D. Walsh, J. Chem. Soc. **1953**, 2266.
[36] H. Biehl, K. J. Boyle, R. P. Tuckett, H. Baumgärtel, and H. W. Jochims, Chem. Phys. **214**, 367 (1997).
[37] S. Koda, J. Phys. Chem. **83**, 2065 (1979).